

# RSC Advances



This is an *Accepted Manuscript*, which has been through the Royal Society of Chemistry peer review process and has been accepted for publication.

*Accepted Manuscripts* are published online shortly after acceptance, before technical editing, formatting and proof reading. Using this free service, authors can make their results available to the community, in citable form, before we publish the edited article. This *Accepted Manuscript* will be replaced by the edited, formatted and paginated article as soon as this is available.

You can find more information about *Accepted Manuscripts* in the [Information for Authors](#).

Please note that technical editing may introduce minor changes to the text and/or graphics, which may alter content. The journal's standard [Terms & Conditions](#) and the [Ethical guidelines](#) still apply. In no event shall the Royal Society of Chemistry be held responsible for any errors or omissions in this *Accepted Manuscript* or any consequences arising from the use of any information it contains.

Cite this: DOI: 10.1039/c0xx00000x

www.rsc.org/xxxxxx

ARTICLE TYPE

## Ultra-sensitive polyaniline-iron oxide nanocomposite room temperature flexible ammonia sensor

D. K. Bandgar,<sup>a</sup> S. T. Navale,<sup>ab</sup> M. Naushad,<sup>c</sup> R.S. Mane,<sup>cd</sup> F. J. Stadler,<sup>b</sup> and V. B. Patil<sup>\*a</sup>

A novel flexible, ultra-sensitive, selective, and room temperature operable polyaniline/iron-oxide (PAni/ $\alpha$ -Fe<sub>2</sub>O<sub>3</sub>) nanocomposite ammonia (NH<sub>3</sub>) gas sensor was developed onto a flexible polyethylene terephthalate (PET) substrate by *in-situ* polymerization process. The observations were recorded to 100ppm fixed level for various gases including NO<sub>2</sub>, CH<sub>3</sub>OH, C<sub>2</sub>H<sub>5</sub>OH, NH<sub>3</sub>, and H<sub>2</sub>S through monitoring the change in resistance of the developed sensor. The flexible PAni/ $\alpha$ -Fe<sub>2</sub>O<sub>3</sub> nanocomposite sensor demonstrated better selectivity towards NH<sub>3</sub> (response = 39% and stability = 74%). The synergistic response of the flexible PAni/ $\alpha$ -Fe<sub>2</sub>O<sub>3</sub> sensor was remarkable than that of the PAni and  $\alpha$ -Fe<sub>2</sub>O<sub>3</sub> alone; indicating the effective improvement in the performance of PAni flexible sensor on nanocomposite process. Moreover, the flexible sensor detected NH<sub>3</sub> at low concentration (5ppm) with a fast response (27s) and very short recovery time (46s). Further, PAni/ $\alpha$ -Fe<sub>2</sub>O<sub>3</sub> flexible sensor films were characterized by X-ray diffraction, field-emission scanning electron microscopy, UV-visible and Raman spectroscopy, Fourier transform infrared and X-ray photoelectron for structural analysis, morphological evolution, optical and surface related studies.

## 1. Introduction

Detecting ammonia (NH<sub>3</sub>) gas at its low level has attracted considerable attention due to its toxicity and its impact on living organisms. According to the US Environmental Protection Agency, a concentration of NH<sub>3</sub> above 25 ppm creates health issues. Therefore, it is essential to develop an NH<sub>3</sub> sensor which is reliable and inexpensive for detecting below the toxic limit. Recently, flexible substrate sensor has been attracting considerable attention<sup>1</sup> due to its interesting characteristics, such as softness, lightness, flexibility and shock resistivity. In general, gas sensors require high temperature to operate effectively and efficiently (>200°C). This is above the continuous operating temperature of most of the polymers, thus, limiting their direct application.<sup>2</sup> So fabricating a sensor, operating at low-temperature i.e. room ( $\leq 45^\circ\text{C}$ ), not only avoids the heating assembly but also makes the sensor setup simpler, portable, and cheaper.<sup>3</sup> Most of the conducting polymers (e.g. polyaniline (PAni), polypyrrole, polythiophene etc.) demonstrate potential gas sensing properties.<sup>4-6</sup> Their advantages include low cost, flexibility in design, tunability, low power consumption and excellent performance at room temperature<sup>7, 8</sup> etc. PAni is one of the scientifically potential polymers with versatile applications including gas sensors and emerged as a star material in the field electrochemical sciences because of its intriguing properties such as high conductivity, good environmental stability, ease of preparation methods etc. Furthermore, PAni can be facilely oxidised and reduced; making it suitable for gas sensing application.<sup>9, 10</sup>

The presence of -NH- group in PAni favours the oxidation, reduction and various physical and chemical properties.<sup>11-13</sup> Besides the sensing capabilities, it can also be used in rechargeable batteries<sup>4, 14</sup>, supercapacitors<sup>15</sup>, light emitting diodes<sup>16</sup>, corrosion protection systems<sup>17</sup>, and electrochromic display devices.<sup>18</sup> But, PAni suffers from a major disadvantage of poor chemical solubility in organic solvents and also hurdles while operating at higher temperatures, limiting its applications. Most semiconducting metal oxide-based gas sensors (tin oxide, zinc oxide, nickel oxide, tungsten oxide and iron oxide etc.) are widely used as a chemiresistive type gas sensors, alternative to conducting polymers due to their ability to detect various gases, high sensitivity, fast response, recovery time and low cost. Most of the metal oxides are *n*-type semiconductors, because electrons are naturally produced due to adsorption of O<sup>2-</sup> during oxide formation.<sup>19</sup> The major disadvantage of metal oxide gas sensors is the need of high temperature. For example, iron oxide (Fe<sub>2</sub>O<sub>3</sub>) used for nitrogen dioxide (NO<sub>2</sub>) sensing required >250°C for a better selectivity<sup>20</sup>, a CdO-Fe<sub>2</sub>O<sub>3</sub> ethanol sensor activated at 300°C.<sup>21</sup> This demands a low-temperature controlled heating system to operate the sensor, as sensor operation at elevated temperature causes gradual changes in the physical and chemical properties of sensor, which promotes deviation in gas sensing properties of sensor with respect to time.

To overcome this difficulty, new prospects can be opened by designing the flexible sensor based on organic-inorganic composite nanostructures. The inorganic materials are thermally more stable as compared to organic i.e. polymer matrices and can improve the sensing characteristics such as sensitivity, selectivity, stability of polymer.<sup>22-25</sup> The most important advantage of organic-inorganic composite nanostructures is that, by combining individual materials different property profiles leads to produce desirable properties in composites. The physicochemical properties of organic-inorganic hybrid nanocomposites depend on the distribution of filler particles into polymer matrix as well as on interfacial bonding between the inorganic filler and polymer matrix. Khuspe *et al.* reported that the incorporation of metal oxides into polymer matrix greatly modify the microstructure and

<sup>a</sup>Functional Materials Research Laboratory (FMRL), School of Physical Sciences, Solapur University, Solapur-413 255, M.S., India. Tel: +912172744770 (Ext-202), E-mail: [drybpatil@gmail.com](mailto:drybpatil@gmail.com), <sup>b</sup>Shenzhen University, Nanshan District Key Lab for Biopolymers and Safety Evaluation, College of Materials Science and Engineering, Shenzhen, Guangdong, China, <sup>c</sup>Department of Chemistry, College of Science, Bld#5, King Saud University, Riyadh, Saudi Arabia, <sup>d</sup>School of Physical Sciences, Swami Ramanand Teerth Marathwada University Nanded-431606, India.

the mechanical properties of original polymer<sup>26</sup> and improves the sensing performance of sensor.<sup>27</sup>

In the present study, PANi was functionalized with  $\alpha$ -Fe<sub>2</sub>O<sub>3</sub> to acclimatize its structural properties and to boost its gas sensing performance in order to induce stronger and faster chemical reactions between PANi sensor and target gas. It is worth noticing that the properties of  $\alpha$ -Fe<sub>2</sub>O<sub>3</sub> not only make them a new class of composites, but also make them capable for reinforcement of fillers within a host PANi matrix.<sup>28</sup> The effect of  $\alpha$ -Fe<sub>2</sub>O<sub>3</sub> filler particles on gas sensing properties of PANi was studied in terms of change in sensor resistance, sensor response, response/recovery time and stability etc. We believe, the unique physical and chemical properties of PANi/ $\alpha$ -Fe<sub>2</sub>O<sub>3</sub> nanocomposite enabling sensing activity at lower concentration of NH<sub>3</sub> gas. PANi/ $\alpha$ -Fe<sub>2</sub>O<sub>3</sub> composite flexible sensor was fabricated by *in-situ* polymerization process using aniline as monomer. *In-situ* polymerization is an excellent approach to form homogenous mixture of two materials. This is simple, low-cost and time saving process and a fine clad of different materials with conducting polymers can be designed on flexible substrates.<sup>29</sup>

## 2. Experimental details

### 2.1 Chemicals used

Ferric chloride hexahydrate (FeCl<sub>3</sub>)<sub>6</sub>H<sub>2</sub>O purchased from Aldrich was used for preparation of iron oxide, methanol was purchased from s-d fine chemicals, aniline as monomer and ammonium persulphate as an oxidant, all are AR grade purchased and were used as received. Polyethylene terephthalate (PET) substrates of the dimensions of 60mm×20mm with ±80µm thickness were purchased and used as it is without any physical and processing.

### 2.2 Fabrication of flexible PANi/ $\alpha$ -Fe<sub>2</sub>O<sub>3</sub> sensor films

Chemically adapted PANi/ $\alpha$ -Fe<sub>2</sub>O<sub>3</sub> nanocomposite flexible sensors were prepared on flexible PET by *in-situ* polymerization process using aniline as monomer and ammonium persulphate as an oxidant in HCl solution; resulting procedure is as follows; 0.1 M APS (Ammonium Per Sulphate) [(NH<sub>4</sub>)<sub>2</sub>S<sub>2</sub>O<sub>8</sub>] was added in 0.2 M aniline (C<sub>6</sub>H<sub>5</sub>NH<sub>2</sub>) and 0.2 M HCl (Hydrochloric Acid) mixture. The resulting mixture was kept at room temperature for 3 h followed by continuous stirring. After polymerization, green precipitate was occurred and is nothing but the emeraldine salt form of PANi. To get emeraldine base form of PANi; de-doping of salt form takes place with 0.1 M NH<sub>4</sub>OH solution and at same time PET substrates were vertically dipped in the beaker.  $\alpha$ -Fe<sub>2</sub>O<sub>3</sub> nanoparticles were synthesized using sol-gel method and incorporated into PANi matrix during de-doping of PANi from 10 to 50 Wt.% (1-5 mass %). After 3 h, blue thin layer of PANi deposited on the PET substrate. The resulting film was washed in distilled water to eliminate the low molecular weight organic intermediates and dried at the ambient temperature and used for further studies. The synthesis process for the development of PANi/ $\alpha$ -Fe<sub>2</sub>O<sub>3</sub> nanocomposite on PET substrate is illustrated through Scheme 1.<sup>26, 29</sup>

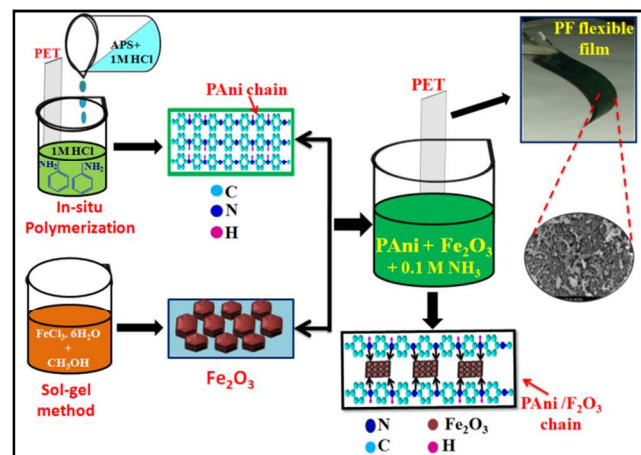
### 2.3 Characterizations and gas sensing measurements

X-ray diffraction (XRD) pattern was recorded on Rigaku Altima-IV diffractometer using Cu-K<sub>α</sub> radiation with a wavelength 1.5406Å in continuous scan mode at an acceleration voltage of 40kV and current of 40mA. The composite formation and bonding characteristics were investigated by a Nicolet IS-10

(Thermo Fischer Scientific Instruments) Fourier transform infrared spectroscopy (FTIR) spectra. The surface morphology of flexible nanocomposite sensor film was analysed by field-emission scanning electron microscopy digital photomicrographs (Model: MIRA3 TESCAN, USA). The interaction of  $\alpha$ -Fe<sub>2</sub>O<sub>3</sub> with PANi was confirmed by UV-visible spectroscopy. The effect of addition of  $\alpha$ -Fe<sub>2</sub>O<sub>3</sub> on polyaniline was investigated by Raman spectroscopy (Model: Horiba, 228 Lab Ram Hr 800). The electrochemical impedance spectroscopy (Precision Impedance Analyzer 6500B) measurement was used to quantify the sensor response to the gases tested. X-ray photoelectron spectroscopy (XPS, VG, Multilab 2000, Thermo VG, Scientific UK) spectra was carried out to investigate the structure of core-level electron and to resolve binding energies of PANi/ $\alpha$ -Fe<sub>2</sub>O<sub>3</sub> nanocomposite. Gas sensing properties were studied using a home-made gas sensor unit equipped with computer-attached KEITHLEY 6514 Electrometer. The NH<sub>3</sub>, nitrogen dioxide (NO<sub>2</sub>), methanol (CH<sub>3</sub>OH), ethanol (C<sub>2</sub>H<sub>5</sub>OH) and liquefied petroleum gases (LPG) etc., have been purchased from space cryo gases Pvt. Ltd., Mumbai. The resultant sensitivity of composite flexible sensor was expressed according to following equation defining the response.

$$\text{Response (\%)} = \frac{|R_a - R_g|}{R_a} \times 100 \quad \dots (1)$$

where R<sub>a</sub> and R<sub>g</sub> are resistances of film sensor in air and target gas, respectively.



**Scheme 1:** Schematic representation of synthesis route of PANi/Fe<sub>2</sub>O<sub>3</sub> nanocomposite on PET substrate by *in-situ* oxidative polymerization.

## 3. Results and discussion

### 3.1 Structural identification

Fig.1 shows the XRD patterns of as-synthesized PANi,  $\alpha$ -Fe<sub>2</sub>O<sub>3</sub> and PANi/ $\alpha$ -Fe<sub>2</sub>O<sub>3</sub> nanocomposite flexible films. From the XRD pattern of pure PANi, single broad peak (Fig.1(a)) in the range of 20-30°(2θ) was evidenced which was higher in enclosed area and intensity, but in the case of composite i.e. PANi/ $\alpha$ -Fe<sub>2</sub>O<sub>3</sub>, several new planes were evidenced. The broad nature of XRD pattern clearly indicated amorphous behavior of synthesized PANi. XRD pattern of  $\alpha$ -Fe<sub>2</sub>O<sub>3</sub> is shown in Fig.1(b). It is noteworthy that high intense XRD peak of PANi at 25.82° is disappeared for composite structure. Shift in XRD peak of PANi in composite structure is eccentric. However, there are few reported wherein

shift of PANi XRD peak position is evidenced when composite is formed<sup>30</sup>, but in present case we believe it could be due to a change of its structure when composite is formed and obtained small intense PANi XRD peak might be a shoulder of previously found broad intense peak. The other peaks of PANi/ $\alpha$ -Fe<sub>2</sub>O<sub>3</sub> composite were similar to the peaks observed in XRD pattern of  $\alpha$ -Fe<sub>2</sub>O<sub>3</sub><sup>27</sup>, confirming the type of  $\alpha$ -Fe<sub>2</sub>O<sub>3</sub> crystal structure which was well-maintained after preparing composite in base media. The XRD result showed the presence of two different phases i.e. PANi and  $\alpha$ -Fe<sub>2</sub>O<sub>3</sub>, supporting for the formation of PANi/ $\alpha$ -Fe<sub>2</sub>O<sub>3</sub> nanocomposite.

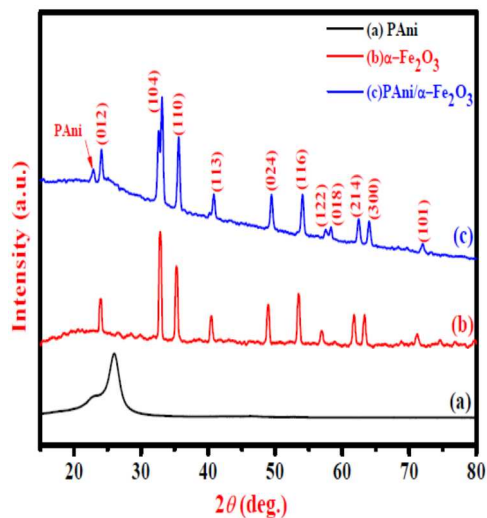


**Fig.1:** XRD patterns of; (a) PANi, (b)  $\alpha$ -Fe<sub>2</sub>O<sub>3</sub>, and (c) PANi/ $\alpha$ -Fe<sub>2</sub>O<sub>3</sub> nanocomposite films.

### 3.2 Surface analysis

To identify the presence of  $\alpha$ -Fe<sub>2</sub>O<sub>3</sub> in the composite and to observe the association between the PANi and the  $\alpha$ -Fe<sub>2</sub>O<sub>3</sub>, FTIR spectra of flexible PANi and PANi/ $\alpha$ -Fe<sub>2</sub>O<sub>3</sub> nanocomposite films were recorded. The peak at 569 cm<sup>-1</sup>, characteristic of the Fe-O stretching vibration, clearly supported for the presence of  $\alpha$ -Fe<sub>2</sub>O<sub>3</sub> in PANi matrix and shift of peak suggested the interaction of  $\alpha$ -Fe<sub>2</sub>O<sub>3</sub> with polyaniline.<sup>31-33</sup> The peak observed (fig.2 (a)) at wave numbers 672 cm<sup>-1</sup> and 736 cm<sup>-1</sup> were attributed to C-H out of plane bending vibrations.<sup>34</sup> The peak at 856 cm<sup>-1</sup> was the characteristic of C-C and C-H for benzenoid ring occurred from C-H out of plane bending vibration of benzene ring.<sup>35-38</sup> The absorption peak at 1061 cm<sup>-1</sup> was due to C-H bending.<sup>35</sup> Also the peak observed at 1283 cm<sup>-1</sup> was on account of C-N stretching of primary aromatic amine ring and the peak observed at 1490 cm<sup>-1</sup> was assigned to C=N stretching in aromatic ring.<sup>39</sup> The peak at 1442 cm<sup>-1</sup> was in favour of C=C stretching mode of benzenoid ring which was shifted to 1450 cm<sup>-1</sup> on addition of  $\alpha$ -Fe<sub>2</sub>O<sub>3</sub>.<sup>40, 41</sup> The absorption peak at 1591 cm<sup>-1</sup> was due to C-C stretching vibration<sup>42</sup> and peak at 1723 cm<sup>-1</sup> was due to C=O bond stretching vibration.<sup>43</sup> Comparing the FTIR spectra of PANi and PANi/ $\alpha$ -Fe<sub>2</sub>O<sub>3</sub> composite, it was concluded that the most of the peaks of PANi were shifted towards higher wavenumber side i.e. PANi/ $\alpha$ -Fe<sub>2</sub>O<sub>3</sub> composite (fig.2 (b)) which could be due to an interaction between PANi and  $\alpha$ -Fe<sub>2</sub>O<sub>3</sub><sup>35</sup> as when nanoparticles of metal oxide are incorporated into a polymer matrix so as to obtain chemically, environmentally and thermally stable composite material, the constituents demonstrate strong

intermolecular interactions, resulting in change of electron density distribution followed FTIR shift.<sup>27</sup>

### 3.3 Raman shift analysis

Chemical structures of PANi and PANi/ $\alpha$ -Fe<sub>2</sub>O<sub>3</sub> nanocomposite flexible films were studied by Raman spectroscopy. Raman spectra of pure PANi (fig.2 (c)) showed the characteristic band at 1175 cm<sup>-1</sup> due to C-H stretching<sup>44</sup>, 1458 cm<sup>-1</sup> due to C=N vibration of quinoid ring<sup>45</sup> and band at 1553 cm<sup>-1</sup> was lined to N-H bending.<sup>46</sup> Raman spectra of PANi/ $\alpha$ -Fe<sub>2</sub>O<sub>3</sub> (fig.2 (d)) composite noted a characteristic band of  $\alpha$ -Fe<sub>2</sub>O<sub>3</sub> at 283 cm<sup>-1</sup>. Bands of pure PANi at 1458 cm<sup>-1</sup> and 1553 cm<sup>-1</sup> shifted in the vicinity of 1304 cm<sup>-1</sup> and 1578 cm<sup>-1</sup> when  $\alpha$ -Fe<sub>2</sub>O<sub>3</sub> was introduced. The shifting of the band was due to a strong mutual interaction of hydrogen bonding between Fe-O of  $\alpha$ -Fe<sub>2</sub>O<sub>3</sub> and -NH- group of PANi.

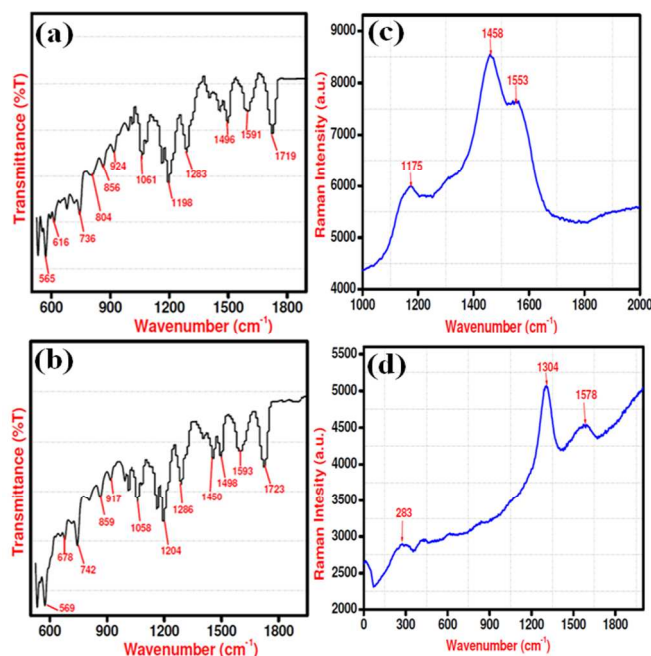


**Fig.2 :** (a, b) FTIR, and (c, d) Raman spectrums of PANi, and PANi/ $\alpha$ -Fe<sub>2</sub>O<sub>3</sub> nanocomposite film surfaces.

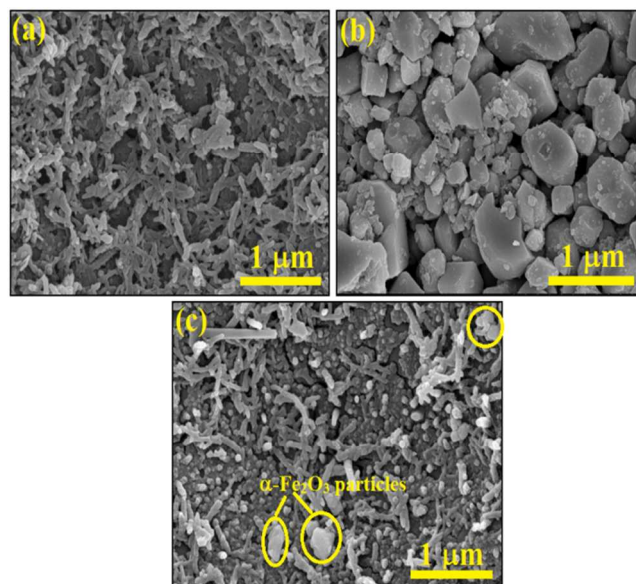
### 3.4 Surface morphological studies

Figure 3 shows the FE-SEM digital micrographs of PANi,  $\alpha$ -Fe<sub>2</sub>O<sub>3</sub>, and PANi/ $\alpha$ -Fe<sub>2</sub>O<sub>3</sub> nanocomposite flexible films prepared by *in-situ* polymerization process. FE-SEM micrograph of PANi (Fig.3 (a)) presents well-grown interconnected fibres of nearly identical diameter, covered uniformly the surface of flexible film. All fibres were porous in surface morphology. Fig.3 (b) shows the FE-SEM micrograph of Fe<sub>2</sub>O<sub>3</sub> film prepared from a powder annealed at 700°C. The particles were elongated-type with few reminiscence of the hexagonal corundum structure of  $\alpha$ -Fe<sub>2</sub>O<sub>3</sub>.  $\alpha$ -Fe<sub>2</sub>O<sub>3</sub> nanoparticles were embedded within the net like structure consisting of PANi fibres in the case of PANi/ $\alpha$ -Fe<sub>2</sub>O<sub>3</sub> composite, suggesting a significant change in the original individual morphologies. As a consequence, PANi/ $\alpha$ -Fe<sub>2</sub>O<sub>3</sub> composite film (Fig.3 (d)) possessed both well-defined forms i.e. PANi and  $\alpha$ -Fe<sub>2</sub>O<sub>3</sub>, implying a highly micro-porous structure and providing a path for insertion and extraction of gas molecules and ensuring high rate of reaction.



### 3.5 Surface analysis

An XPS spectrum was employed to analyse the effect  $\alpha$ -Fe<sub>2</sub>O<sub>3</sub> and to understand the different electronic structures and chemical bonding information of PANi/ $\alpha$ -Fe<sub>2</sub>O<sub>3</sub> composite. XPS core level spectrum of PANi/ $\alpha$ -Fe<sub>2</sub>O<sub>3</sub> nanocomposite demonstrated C1s, O1s, N1s and Fe 2p peaks, which were related to the binding energies of C, O, N, and Fe, respectively. Fig. 4(a) presents the C1s core-level spectrum of PANi/ $\alpha$ -Fe<sub>2</sub>O<sub>3</sub> composite; deconvoluted into three components at binding energies 283.8eV, 285.85eV and 287.7eV, respectively. Peak assigned at binding energy 283.8eV was due to C-H band.<sup>47</sup> The peaks observed at binding energy 285.85eV and 287.7eV were attributed to C-N and C=O band, respectively.<sup>47</sup> Core-level O 1s in XPS spectrum of PANi/ $\alpha$ -Fe<sub>2</sub>O<sub>3</sub> nanocomposite highlighted in Fig. 4(b). The spectrum deconvoluted into three components; peak observed at lower binding energy (530eV) was the characteristic peak of  $\alpha$ -Fe<sub>2</sub>O<sub>3</sub>, which was attributed to O-H band.<sup>48,49</sup> The peak observed at 531.9eV was assigned to surface oxygen due to chemisorbed water<sup>49,50</sup> and the peak evidenced at higher binding energy (533.4eV) was due to oxygen within the Fe-O-H bond because the estimated binding energy of O 1s electron for adsorbed water is 533eV.<sup>49</sup> N1s core-level spectrum of PANi/ $\alpha$ -Fe<sub>2</sub>O<sub>3</sub> nanocomposite is shown in Fig. 4(c). The N1s core-level spectrum was situated around a binding energy of 399.4eV, indicating the existence of benzenoid ring in the PANi/ $\alpha$ -Fe<sub>2</sub>O<sub>3</sub> nanocomposite as well as the prepared PANi could be in the neutral media with emeraldine form.<sup>51,52</sup> Fig. 4(d) shows the core-level spectrum of Fe with two peaks located at binding energies of 710.85 eV (Fe<sup>3+</sup> state) and 724.35 eV, respectively, and were well-matched with values reported in literature.<sup>49,53</sup> These observed bands indicated the presence of inorganic phase of  $\alpha$ -Fe<sub>2</sub>O<sub>3</sub> in the composite.<sup>49</sup>



**Fig.3:** FESEM micrographs of; (a) PANi, (b)  $\alpha$ -Fe<sub>2</sub>O<sub>3</sub>, and (c) PANi/ $\alpha$ -Fe<sub>2</sub>O<sub>3</sub> composite films.

### 3.6 Gas sensing studies

#### 3.6.1 Selectivity

High selectivity is an important parameter for excellent working of sensor. To confirm the selectivity of the sensor to a particular

gas, chemo-resistive properties were studied for PANi and PANi/ $\alpha$ -Fe<sub>2</sub>O<sub>3</sub> nanocomposite sensors by exposing sequentially for different gases. Selectivity study of PANi/ $\alpha$ -Fe<sub>2</sub>O<sub>3</sub> nanocomposite sensor was performed for NH<sub>3</sub>, H<sub>2</sub>S, C<sub>2</sub>H<sub>5</sub>OH, CH<sub>3</sub>OH, and NO<sub>2</sub> at 100 ppm concentration of each gas and given in Fig. 5(a). Resistance of PANi film sensor was not changed to C<sub>2</sub>H<sub>5</sub>OH and CH<sub>3</sub>OH gases, hence, the response was considered to be zero, confirming that these gases are not interacting with the PANi sensor. But when PANi sensor was exposed to NO<sub>2</sub> and H<sub>2</sub>S gases, responses were increased by 1% and 0.5%, respectively; considerably lower as compared to NH<sub>3</sub> (26%) gas. Selectivity study clearly supported that, PANi/ $\alpha$ -Fe<sub>2</sub>O<sub>3</sub> sensor was more selective to NH<sub>3</sub> than other test gases and exhibited higher selectivity to NH<sub>3</sub> when compared to pure PANi. After addition of  $\alpha$ -Fe<sub>2</sub>O<sub>3</sub> nanoparticles in PANI matrix, quinoid structure (higher conjugation) of PANi was transformed into benzoid structure (lower conjugation) and made it more selective to target gas (herein NH<sub>3</sub>).<sup>5</sup>

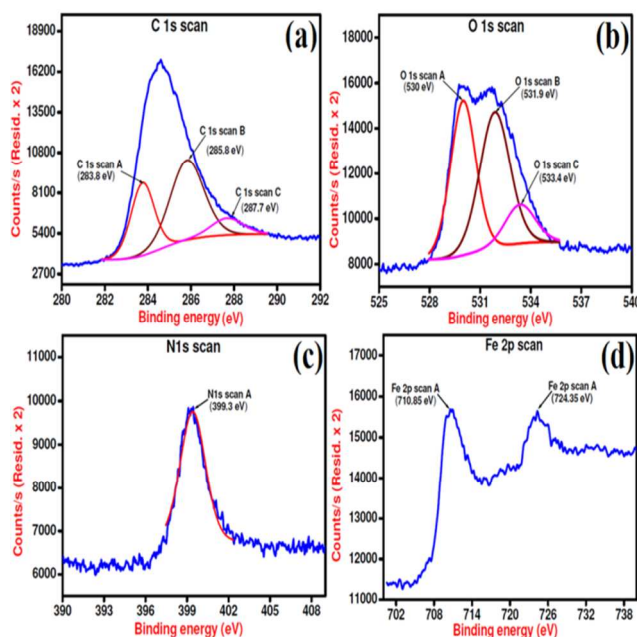


**Fig.4:** (a) C 1s, (b) O 1s, (c) N 1s, and (d) Fe2p of PANi/ $\alpha$ -Fe<sub>2</sub>O<sub>3</sub> composite.

#### 3.6.2 NH<sub>3</sub> dependent response of PANi/ $\alpha$ -Fe<sub>2</sub>O<sub>3</sub> flexible sensor

NH<sub>3</sub> gas sensing behaviour of PANi/ $\alpha$ -Fe<sub>2</sub>O<sub>3</sub> nanocomposite flexible sensor was determined by monitoring the electrical resistance. At first PANi/ $\alpha$ -Fe<sub>2</sub>O<sub>3</sub> sensor was exposed to air to measure the sensor resistance in air ( $R_a$ ). Fig.5(b) shows the response of flexible PANi/ $\alpha$ -Fe<sub>2</sub>O<sub>3</sub> nanocomposite sensor to NH<sub>3</sub> gas at room temperature. From the response graph, it was observed that the sensor resistance was increased immediately with time when sensor exposed to NH<sub>3</sub> gas. At the beginning when NH<sub>3</sub> gas was injected into the chamber, the measured resistance of sensor increased rapidly, reached to its maximum value and became stable, which was used to define the resistance of sensor in gas ( $R_g$ ). Recovery of sensor was achieved by opening the lead of chamber, leading to a strong gradual decrease of the measured resistance of PANi/ $\alpha$ -Fe<sub>2</sub>O<sub>3</sub> nanocomposite sensor until reaching to its initial value  $R_a$ . Decrease in resistance of sensor after exposure to air was due to a decrease of NH<sub>3</sub> concentration.<sup>55</sup> According to equation (1), the response obtained

for PANi/ $\alpha$ -Fe<sub>2</sub>O<sub>3</sub> nanocomposite flexible sensor was 39% for 100ppm level of NH<sub>3</sub> gas with short response (27s) and (46s) recovery times, defined as the time from exposure to NH<sub>3</sub> to the peak in resistance and the time from exposure to pure air till the previous resistance, respectively.

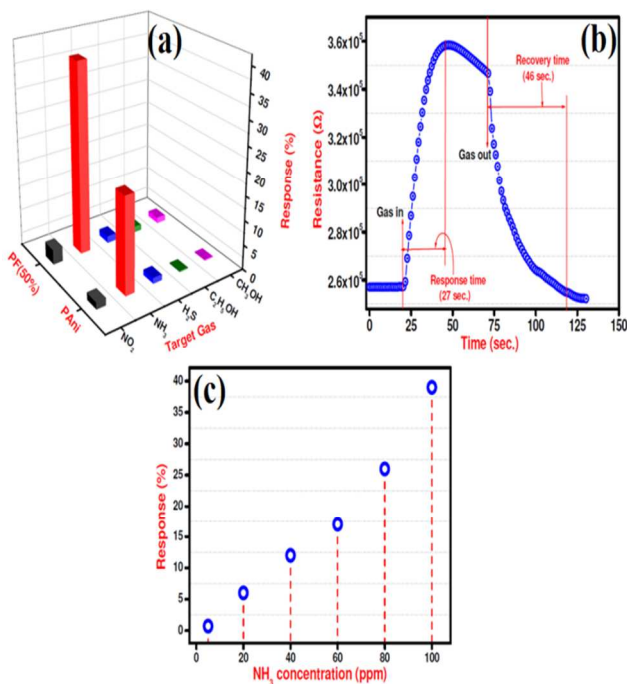
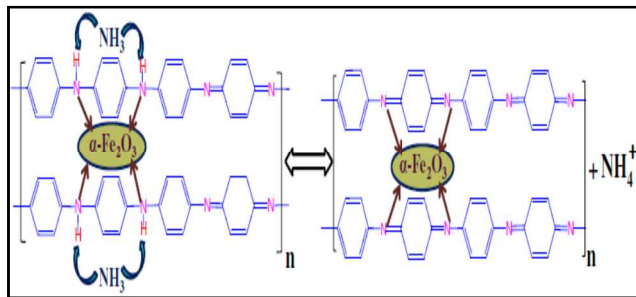


**Fig.5:** (a) Selectivity study of PANi and PANi/ $\alpha$ -Fe<sub>2</sub>O<sub>3</sub> sensor films, (b) Change in resistance as a function of time of PANi/ $\alpha$ -Fe<sub>2</sub>O<sub>3</sub> sensor film upon 100 ppm exposure of NH<sub>3</sub> gas, and (c) Response of flexible composite sensor to different NH<sub>3</sub> concentrations.

### 3.6.3. Gas sensing mechanism

The gas sensing mechanism for PANi/ $\alpha$ -Fe<sub>2</sub>O<sub>3</sub> flexible sensor was straightforwardly concluded to stem from N-H group of PANi, by deprotonation and protonation<sup>56</sup>. Fig.5 (b) shows that the resistance of PANi/ $\alpha$ -Fe<sub>2</sub>O<sub>3</sub> nanocomposite flexible sensor is increased on exposure to NH<sub>3</sub> (electron donor) gas. Similar behaviour of PANi-metal oxide composite sensors for NH<sub>3</sub> gas detection is found in literature for PANi-TiO<sub>2</sub> (Tai *et al.*<sup>12</sup>), PANi-ZnO (Khan *et al.*<sup>13</sup>), PANi-SnO<sub>2</sub> (Khuspe *et al.*<sup>27</sup> and Geng *et al.*<sup>7</sup>) sensors. Being NH<sub>3</sub> as a reducing agent, for *p*-type polyaniline fibres, resistance was increased upon interaction.



**Scheme 2:** Possible sensing mechanism of NH<sub>3</sub> gas with PANi/ $\alpha$ -Fe<sub>2</sub>O<sub>3</sub> film sensor.

During the process NH<sub>3</sub>, as a deprotonating agent, might interact with H<sup>+</sup> ion on the PANi backbone, withdrawing protons from N-H sites followed transferring them to ammonium (NH<sub>4</sub><sup>+</sup>) ions<sup>13</sup> as shown in Scheme 2. After attaining optimum we found there was decrease in resistance before switching gas to its off level within 50-75 s, which was unusual, and might arise from an interaction of NH<sub>3</sub> gas molecules with host material i.e. as NH<sub>3</sub> is electron donating moiety thereby when it interacts with composite thin film which is *p*-type in nature; shift in its Fermi energy level towards conduction band position side with reduced resistivity is anticipated. The increase in electrical resistance was attributed to proton charge transfer from PANi to NH<sub>3</sub> gas.<sup>9,10</sup> Due to loss of H<sup>+</sup> ion, surface depletion region was increased, thereby; the conductivity of PANi was decreased. When sensor film was exposed to air; could capture hydrogen from NH<sub>4</sub><sup>+</sup> and renovate the initial doping level of PANi.<sup>9,10,13</sup> This added H<sup>+</sup>, form N-H bond and thus the resistance of sensor was decreased. However, the mechanism for NH<sub>3</sub> gas molecules and  $\alpha$ -Fe<sub>2</sub>O<sub>3</sub> interactions in composite form was unprecedented. Our previous results showed that, the resistance of  $\alpha$ -Fe<sub>2</sub>O<sub>3</sub> remained unchanged upon exposure to NH<sub>3</sub> gas<sup>57</sup>, suggesting NH<sub>3</sub> can be an inert gas for  $\alpha$ -Fe<sub>2</sub>O<sub>3</sub>.

### 3.6.4 Influence of NH<sub>3</sub> concentration

The performance of PANi/ $\alpha$ -Fe<sub>2</sub>O<sub>3</sub> flexible sensor was determined by measuring the sensor response for different ammonia gas concentrations at room temperature (30°C) (Fig.5(c)), revealing to be sensitive as low as 5ppm of NH<sub>3</sub>. From Fig. 5 (c) it is revealed that, the response of PANi/ $\alpha$ -Fe<sub>2</sub>O<sub>3</sub> sensor was increased with rising NH<sub>3</sub> gas concentration. At higher concentration of ammonia (100 ppm) it showed not only the maximum response (39%) but also very short response time (27 s), with increase of concentration the number of gas molecules interacting with sensor surface increases as well.

### 3.6.5 Reproducibility, response-recovery, stability and impedance studies

Reproducibility study of PANi/ $\alpha$ -Fe<sub>2</sub>O<sub>3</sub> nanocomposite flexible sensor revealed that the sensor maintained its initial amplitude with short response and recovery times for three cycles of NH<sub>3</sub> gas exposure, indicating good stability of sensor [Fig. 6(a)]. Complete recovery of sensor resistance to its initial baseline value after exposition to air, evidencing favourable industrial and market quality of developed sensor. This was due to protonation and deprotonation of polyaniline. Fig.6 (b) shows response vs. recovery time graph of PANi/ $\alpha$ -Fe<sub>2</sub>O<sub>3</sub> flexible sensor to different NH<sub>3</sub> gas concentrations. Very short response time (27 s) and recovery time (46 s) were noted at 100ppm of NH<sub>3</sub> gas concentration. Whereas, at the lowest concentration of NH<sub>3</sub> gas (5 ppm), 76 s response time and 5 s recovery time were recorded, giving an indicator for the speed of the adsorption-desorption of NH<sub>3</sub> gas on the sensor. From the response-recovery observations, it was evident that with increase of the NH<sub>3</sub> gas concentration, response time was decreased drastically and recovery time was increased intensively; faster than previously reported literature values.<sup>35,58</sup> The stability of the sensor was determined by measuring the response of the sensor for every five days for one month [Fig. 6 (c)] by fixing the constant concentration (100ppm) of NH<sub>3</sub> gas, showing a decrease of response for the few first days until reach to an equilibrium level *i.e.* response after 15 days. Hence, PANi/ $\alpha$ -Fe<sub>2</sub>O<sub>3</sub> flexible sensor showed good (74%) long-term stability. The impedance spectra of PANi/ $\alpha$ -Fe<sub>2</sub>O<sub>3</sub> flexible sensor was measured in air and gas at room temperature and

covers in Fig.6 (d). Impedance was measured in the frequency range of 20Hz to 10 MHz; the plot of imaginary component ( $Z''$ ) against the real component ( $Z'$ ) exhibited a perfect semicircle. The series resistance  $R_s$  was found by the value of real impedance at the highest frequency intercept.  $R_1$  and  $C_1$  component in the equivalent circuit correspond to the bulk properties while  $R_2$  and  $C_2$  component correspond to the grain boundary properties of the PANi/ $\alpha$ -Fe<sub>2</sub>O<sub>3</sub>. Table 1 summarizes the values of impedance parameter in air and gas. When the gas was injected in to the chamber resistance  $R_1$  was increased and capacitance  $C_1$  was decreased.

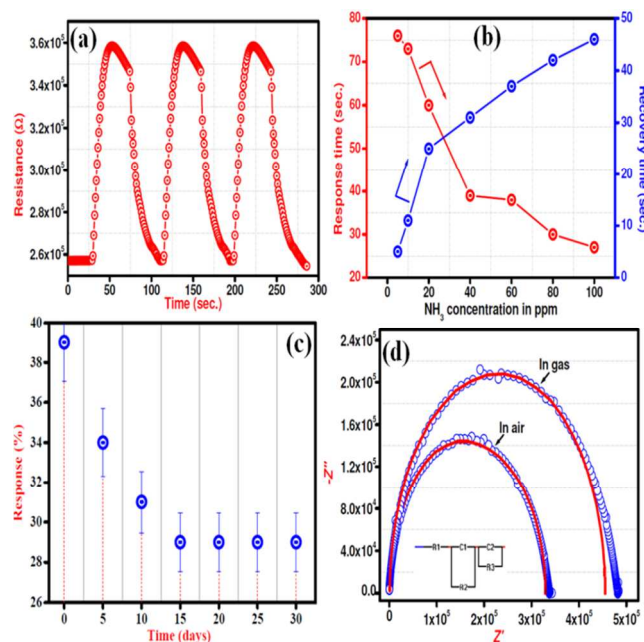


**Fig.6:** (a) Reproducibility, (b) Response vs. recovery variation, (c) Stability of PANi/ $\alpha$ -Fe<sub>2</sub>O<sub>3</sub> nanocomposite sensor, and (d) Impedance spectra ( $Z'$  vs.  $Z''$ ) of PANi/ $\alpha$ -Fe<sub>2</sub>O<sub>3</sub> in presence of air and NH<sub>3</sub> gas. Inset shows an equivalent circuit.

**Table 1:** Impedance parameters for PANi/ $\alpha$ -Fe<sub>2</sub>O<sub>3</sub> flexible nanocomposite sensor.

Parameter	$R_0$ (K $\Omega$ )	$R_1$ (K $\Omega$ )	$R_2$ (K $F$ )	$C_1$ (nF)	$C_2$ (nF)
Air	3	109.80	216.66	1.23	0.21
Gas	3	199.13	254.930	1.15	2.02

#### 4. Conclusions

PANi/ $\alpha$ -Fe<sub>2</sub>O<sub>3</sub> composite ammonia sensor was successfully developed on PET substrate by *in-situ* polymerization method. The resulting composite sensor was a mixture of fibers PANi and crystals of  $\alpha$ -Fe<sub>2</sub>O<sub>3</sub>. There was strong coupling between PANi and  $\alpha$ -Fe<sub>2</sub>O<sub>3</sub> as well as the formation of composite of PANi and  $\alpha$ -Fe<sub>2</sub>O<sub>3</sub>. PANi/ $\alpha$ -Fe<sub>2</sub>O<sub>3</sub> nanocomposite flexible sensors was highly selective to NH<sub>3</sub> gas at room temperature compared to other test gases. The sensor response was measured with the change of resistance which was linearly increased with an increase of NH<sub>3</sub> concentration from 5ppm to 100ppm. The NH<sub>3</sub> sensor showed highest response of 39% with a fast 27s response time and 47s

recovery time at 100ppm of NH<sub>3</sub> gas. Impedance spectra measured in air and gas and was well-fitted by with two time constants in series. Due to the room temperature operation and low development cost, flexible substrate, developed composite sensor can find numerous applications in domestic and industrial market areas from the points of safely, ecology and economy.

#### Acknowledgements

Dr. V. B. Patil would like thank DAE-BRNS, for financial support through the scheme no. 2010/37P/45/BRNS/1442. FJS would like to acknowledge Nanshan District Key Lab for Biopolymers and Safety Evaluation (No.KC2014ZDZJ0001A). The authors would like to extend their sincere appreciation to the Deanship of Scientific Research at King Saud University for funding this work through the Research Group NO. RG-1436-034.

#### References

- G. Rizzo, A. Arena, N. Donato, M. Latino, G. Saitta, A. Bonavita, G. Neri, *Thin Solid Films*, 2010, **518**, 7133.
- M. C. Mcalpine, H. Ahmad, D. Wang, J. R. Heath, *Nat. Mater.*, 2007, **6**, 379.
- A. Arena, N. Donato, G. Saitta, A. Bonavita, G. Rizzo, G. Neri, *Sens. Actu. B*, 2010, **145**, 488.
- X. B. Yan, Z. J. Han, Y. Yang, B. K. Tay, *Sens. Actu. B*, 2007, **23**, 107.
- A. Joshi, D. K. Aswal, S. K. Gupta, J. V. Yakhmi, S. A. Gangal, *Appl. Phys. Lett.*, 2009, **94**, 103115.
- S. T. Navale, A. T. Mane, G. D. Khuspe, M. A. Chougule, V. B. Patil, *Synt. Met.*, 2014, **195**, 228.
- L. Geng, Y. Zhao, X. Huang, S. Wang, S. Zhang, S. Wu, *Sens. Actu. B*, 2007, **120**, 568.
- S.T. Navale, A. A. Ghanwat, V. B. Patil, *Measurement*, 2014, **50**, 363
- R. G. Bavane, A. M. Mahajan, M. D. Shirsat, R. B. Gore, *J. Adv. Phys.*, 2013, **3**, 241.
- M. Matsuguchi, J. Io, G. Sugiyama, Y. Sakai, *Synt. Met.*, 2002, **128**, 15.
- D. N. Debarnot, F. P. Epailard, *Anal. Chimica Acta*, 2003, **475**, 1.
- H. Tai, Y. Jiang, G. Xie, J. Yu, X. Chen, *Sens. Actu. B*, 2007, **125**, 644.
- A. A. Khan, M. Khalid, *J. App. Poly. Sci.*, 2010, **117**, 1601.
- A. Mirmohseni, R. Solhjo, *Eur. Poly. J.*, 2003, **39**, 219.
- M. M. Khandpekar, R. K. Kushwaha, S. P. Pati, *Sol. State Elect.*, 2011, **62**, 156.
- E. Menefee, Y. H. Pao, *J. Chem. Phys.*, 1962, **35**, 3472.
- C. K. Chiang, S. C. Gau, C. R. J. Fincher, Y. W. Park, A. G. MacDiarmid, A. J. Heeger, *Appl. Phys. Lett.*, 1978, **33**, 18.
- R. Dupon, D. H. Whitmore, D. F. Shriver, *J. Elect. Soci.* 1981, **128**, 715.
- K. Wetchakun, T. Samerjai, N. Tamaekong, C. Liewhiran, C. Siri Wong, V. Kruefu, A. Wisitsoraat, A. Tuantranont, S. Phanichphant, *Sens. Actu. B*, 2011, **160**, 580.
- G. Neria, A. Bonavita, S. Galvagno, P. Sicilianob, S. Capone, *Sens. Actu. B*, 2002, **82**, 40.
- X. Liu, Z. Xu, Y. Liu, Y. Shen, *Sens. Actu. B*, 1998, **52**, 270.
- M. A. D. Paoli, R. J. Waltman, A. F. Diaz, and J. Bargon, *J. Chem. Soc. Chem. Comm.*, 1984, **15**, 1015.
- S. E. Lindsey, S. B. Street, *Synt. Met.*, 1984, **10**, 67.
- C. Cassagnol, M. Cavarero, A. Boudet, A. Ricard, *Polymer*, 1999, **40**, 1139.



- 25 N. V. Bhat, A. P. Gadre, V. A. Bambole, *J. Appl. Polym. Sci.*, 2001, **80**, 2511.
- 26 S. Bai, Y. Zhao, J. Sun, Y. Tian, R. Luo, D. Li, A. Chen, *Chem. Comm.*, 2012, **00**, 1
- 5 27 G.D. Khuspe, S. T. Navale, D. K. Bandgar, R. D. Sakhare, M. A. Chougule, V. B. Patil, *Elect. Mat.Lett.*, 2014, **10**, 191.
- 28 Y. Wu, S. Xing, S. Jing, T. Zhou, C. Zhao, *e-Polymers*, 2007, **103**, 1.
- 29 J. Stejskal, I. Sapurina, *Pure & Appl. Chem.*, 2005, **77**, 815.
- 10 30 S.Wang, Y. Hua, R. Zonga, Y. Tanga, Z. Chenb, W. Fana, *Appl. Clay Sci.*, 2004, **25**, 49.
- 31 C. Yang, J. Du, Q. Peng, R. Qiao, W. Chen, C. Xu, Z. Shuai, M. Gao, *J. Phys. Chem. B*, 2009, **113**, 5052.
- 32 V. A. Khatil, S. B. Kondawar, V. A. Tabhane, *Anal. Bioanal. Electro.*, 2011, **3**, 614.
- 15 33 K. R. Reddy, K. P. Lee, A. I. Gopalan, *J. App. Poly. Sci.*, 2007, **106**, 1181.
- 34 R. Hawaldar, M. Kulkarni, S. Jadkar, U. Pal, D. Amalnerkar, *J. Nano. Res.*, 2009, **5**, 79.
- 20 35 J. Husain, S. B. Chacradhar, M. V. N. Ambika Prasad, *Int. J. Eng. Res. Appl.*, 2014, **4**, 198.
- 36 N. G. Deshpande, Y. G. Gudage, R. Sharma, J. C. Vyas, J. B. Kim, Y. P. Lee, *Sens. Actua. B*, 2009, **138**, 76.
- 37 A. H. Elsayed, M. S. MohyEldin, A. M. Elsyed, A. H. Abo Elazm, E. M. Younes, H. A.Motaweh, *Int. J. Electrochem. Sci.*, 2011, **6**, 206.
- 25 38 P. Kunzo, P. Lobotka, E. Kovacova, K. Chrissopoulou, L. Papoutsakis, S. H. Anastasiadis, Z. Krizanova, I. Vavra, *Phys. Stat. Sol. A*, 2013, **210**, 2341.
- 30 39 J. Vivekanandan, V. Ponnusamy, A. Mahudeswaran, P. S. Vijayanand, *Arch. Appl. Sci. Res.*, 2011, **3**, 147.
- 40 A. Khan, A. S. Aldwayyan, M. Alhoshan, M. Alsalhi, *Polym. Int.*, 2010, **59**, 1690.
- 41 T. H. Hsieh, K. S. Ho, C. H. Huang, Y. Z. Wang, Z. L. Chen, *Synth. Met.*, 2006, **156**, 1355.
- 35 42 S. T. Navale, G. D. Khuspe, M. A. Chougule, V. B. Patil, *J. Phy. Chem. Sol.*, 2014, **75**, 236.
- 43 M. R. Saboktakin, A. Maharramov, M. A. Ramazanov, *Nat. Sci.*, 2007, **5**, 67.
- 40 44 B. E. J. Tabares, F. J. Isaza, S. I. Cordoba de Torresi, *Mat. Chem. Phy.*, 2012, **132**, 529.
- 45 R. Mazeikiene, G. Niaura, A. Malinauskas, *Electrochimia. Acta*, 2006, **51**, 5761.
- 46 R. Mazeikiene, V. Tomkute, Z. Kuodis, G. Niaura, A. Malinauskas, *Vibra. Spectro.*, 2007, **44**, 201.
- 45 47 M. G. Han, S. S. Im, *Polymer*, 2000, **41**, 3253.
- 48 G. Wang, Y. Ling, D. A. Wheeler, K. E. N. George, K. Horsley, C. Heske, J. Z. Zhang, Y. Li, *Nano Lett.*, 2011, **11**, 3503.
- 50 49 P. Mills, J. L. Sullivan, *J. Phys. D: Appl. Phys.*, 1983, **16**, 723.
- 50 G. Wu, X. Tan, G. Li, C. Hu, *J. Alloys Comp.*, 2010, **504**, 371.
- 51 G. Qiu, Q. Wang, M. Nie, *J. Appl. Poly. Sci.*, 2006, **102**, 2107.
- 55 52 L. Konga, X. Lub, W. Zhang, *J. Sol. State Chem.*, 2008, **181**, 628.
- 53 S. Liu, D. Tao, L. Zhang, *Powder Tech.*, 2012, **217**, 502.
- 54 A. Z. Sadek, W. Wlodarski, K. Shin, R. B. Kaner, K. Kalantar-zadeh, *Nanotechnol.*, 2006, **17**, 4488.
- 60 55 S. K. Shukla, N. B. Singh, R.P. Rastogi, *Ind. J. of Eng. Mat. Sci.*, 2013, **20**, 319.
- 56 R. Arora, A. Srivastav, U. K. Mandal, *Int. J. Mod. Eng. Res.*, 2012, **2**, 2384.
- 65 57 S. T. Navale, D. K. Bandgar, S. R. Nalage, G. D. Khuspe, M. A. Chougule, Y. D. Kolekar, S. Sen, V. B. Patil, *Ceram. Int.*, 2013, **39**, 6453.
- 58 S. Srivastava, S. Kumar, Y. K. Vijay, *Int. J. Hydro. Energy*, 2012, **37**, 3825.



## Ultra-sensitive polyaniline-iron oxide nanocomposite room temperature flexible ammonia sensor

We report for the first time a room temperature smart  $\text{NH}_3$  sensor based on PANi- $\text{Fe}_2\text{O}_3$  nanocomposite loading on flexible PET substrate by in-situ chemical oxidative polymerization method. The sensor not only exhibits high sensitivity, good selectivity and fast response but also has flexibility, cheap and wearable features.

